

Study of 1^+ States in $^{48}\text{V}^\dagger$ J. W. Smith,* L. Meyer-Schützmeister, and Gerald Hardie‡
Argonne National Laboratory, Argonne, Illinois 60439

and

P. P. Singh
Indiana University, Bloomington, Indiana 47401

(Received 18 June 1973)

15 states in ^{48}V have been studied by means of the $^{46}\text{Ti}(^3\text{He}, p)^{48}\text{V}$ reaction induced by a 17-MeV $^3\text{He}^{++}$ beam from the Argonne tandem Van de Graaff. The proton angular distributions led to the identification of one 0^+ state (the isobaric analog of the ^{48}Ti ground state) and 7 1^+ states. The excitation energies of the 1^+ states are compared with those predicted by a shell-model calculation which assumed a $(\pi f_{7/2})^3(\nu f_{7/2})^{-3}$ configuration. The differential cross sections for populating states in ^{48}V by transferring an n - p pair with 0 or 0 + 2 units of angular momenta are compared with similar cross sections in neighboring nuclei to investigate possible regularities in this mass region. The γ decay of the 0^+ and 1^+ states was determined by studying p - γ coincidences associated with the $^{46}\text{Ti}(^3\text{He}, p\gamma)^{48}\text{V}$ reaction. The γ decay of the 1^+ states shows a definite pattern which is compared with one based on a selection rule involving the signatures of the wave functions describing the 1^+ states.

I. INTRODUCTION

A recent theoretical investigation¹ has shown that M1 transitions between certain states that are describable by the configuration $(\pi f_{7/2})^3(\nu f_{7/2})^{-3}$ are forbidden in the odd-odd cross-conjugate nucleus ^{48}V . This selection rule should influence the γ -decay pattern for the 1^+ states of the $f_{7/2}$ nucleon configuration. To test this expectation experimentally, we identified seven 1^+ states by studying the measured angular distributions of protons from the $^{46}\text{Ti}(^3\text{He}, p)^{48}\text{V}$ reaction and have established their γ -decay patterns by obtaining coincidences between protons and γ rays from this reaction. The measured energies of these states are in good agreement with the energies calculated on the assumption of a pure $f_{7/2}$ nucleon configuration. One therefore hopes that the theoretical calculation will be equally successful in reproducing the measured γ -decay scheme. The theoretical and experimental results will be discussed and compared in the following sections.

II. MAGNETIC SPECTROGRAPH MEASUREMENTS

A. Energy Levels

The nucleus ^{48}V was studied by use of the $^{46}\text{Ti}(^3\text{He}, p)^{48}\text{V}$ reaction. The target was prepared by rolling Ti metal, enriched to 83.6% in ^{46}Ti , to a thickness of 210 $\mu\text{g}/\text{cm}^2$. Proton groups produced when a 17-MeV ^3He beam from the Argonne tandem Van de Graaff struck the target were analyzed in a split-pole magnetic spectrograph² and detected by 50- μm -thick Kodak NTB emulsions covered

with acetate foils to stop unwanted particles. After exposure, the plates were developed and then scanned automatically.³ A spectrum of protons emitted at an angle of 7° to the incoming ^3He beam is shown in Fig. 1. The energy resolution is about 40 keV full width at half maximum (FWHM). (Proton groups are labeled if they are of importance in the discussion, are well isolated, or could be analyzed at most angles by a curve-fitting procedure.) Since the target contains 9.6% ^{48}Ti , weak proton groups are excluded if their Q values are close to those associated with states that are expected⁴ to be strongly populated by the $(^3\text{He}, p)$ reaction on

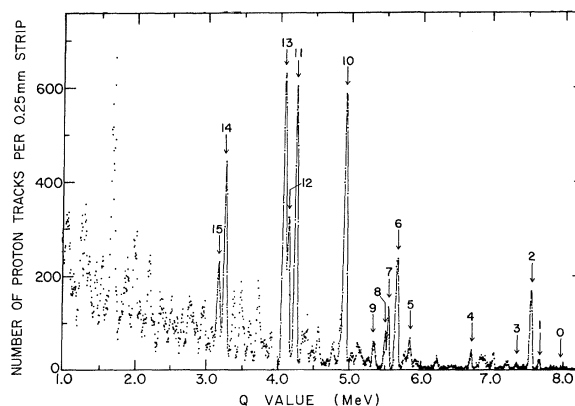


FIG. 1. Spectrum of protons from the $^{46}\text{Ti}(^3\text{He}, p)^{48}\text{V}$ reaction. The measurements were made with split-pole magnetic spectrograph at an angle of 7° to the incoming 17-MeV beam. The target was a rolled ^{46}Ti foil 210 $\mu\text{g}/\text{cm}^2$ thick. The energies of the labeled proton groups are given in Table I, col. 2.

^{48}Ti . The excitation energies of the states in ^{48}V populated by these proton groups are given in Table I, column 2. The energies quoted are derived, when possible, from the γ -decay studies with the $^{46}\text{Ti}(^3\text{He}, p\gamma)^{48}\text{V}$ reaction, the energies^{5, 6} of the first and second excited states being taken as 0.308 and 0.421 MeV, respectively. These energies agree well with those of earlier studies⁷⁻¹⁰ of the $(^3\text{He}, p)$ reaction, as seen in columns 6 and 9 of Table I. In addition, the results from the $^{47}\text{Ti}(^3\text{He}, d)^{48}\text{V}$ reaction¹¹ are given (last four columns) for those states that can be reliably identified with those seen with the $(^3\text{He}, p)$ reaction. The proton group with an excitation energy slightly less than that of state 14 shown in Fig. 1 is the result of two closely spaced levels. Both components have small cross sections and could be analyzed with reasonable accuracy only at a few angles (see Sec. II B).

B. Angular Distributions

Angular distributions, with data points taken at fifteen angles in the range from 7 to 64°, have been obtained for the proton groups from the $^{46}\text{Ti}(^3\text{He}, p)^{48}\text{V}$ reaction. The shapes of many of these angular distributions match those predicted by distorted-

wave Born-approximation (DWBA) calculations, and from this correspondence the orbital angular momentum L_{np} transferred to the target nucleus by the n - p pair can be inferred. The angular distribution of the proton group populating the isobaric analog ($J=0^+$, $T=2$) at 3.019 MeV is seen at the top in Fig. 2. The solid curve represents the angular distribution calculated¹² for an $L_{np}=0$ transfer. The parameters employed in the calculations are given in Table II. They are only slightly different from those used¹³ in the calculations of the angular distributions resulting from the $^{45}\text{Sc}(^3\text{He}, p)^{47}\text{Ti}$ reaction. The two lower distributions in Fig. 2 have shapes characteristic of $L_{np}=2$. The solid curve is the angular distribution calculated for the first excited state ($E_x=0.308$ MeV) on the assumption that $L_{np}=2$.

Seven angular distributions, all very similar, are shown in Fig. 3. At small angles they fall off rather steeply with increasing angle. However, in contrast to the deep minimum in a pure $L_{np}=0$ distribution (solid curve at the bottom of the figure), the minima in these angular distributions are "filled-in." This "filling-in" results from a mixture of $L_{np}=0$ and $L_{np}=2$ transfers. Such distributions from $(^3\text{He}, p)$ reactions on $J=0^+$ targets indicate¹⁴ final states with $J=1^+$. In all but two

TABLE I. Comparison among the present magnetic-spectrograph results, earlier $(^3\text{He}, p)$ studies (Refs. 7-10), and the $(^3\text{He}, d)$ studies of Ref. 11.

Level No.	$^{46}\text{Ti}(^3\text{He}, p)^{48}\text{V}$ (present work)			$^{46}\text{Ti}(^3\text{He}, p)^{48}\text{V}$ ^a			$^{46}\text{Ti}(^3\text{He}, p)^{48}\text{V}$ ^b			$^{47}\text{Ti}(^3\text{He}, d)^{48}\text{V}$ ^c		
	E_x (MeV)	J^π	L_{np}	E_x (MeV)	J^π	L_{np}	E_x (MeV)	J^π	E_x (MeV)	J^π	$[(2J_f+1)/(2J_i+1)]C^2S$ $L_p=3$ $L_p=1$	
0	0.0			0.0	4^+				0.0	4^+	0.33	0.02
1	0.308		2	0.312	2^+	2			0.310	2^+	0.23	(0.004)
2	0.421	1^+	0+2	0.424	1^+	0	0.42	1^+	0.428	1^+	0.87	
3	0.620			0.622					0.616		0.83	
4	1.254			1.252								
5	2.101											
6	2.289	1^+	0+2	163±30	2.296	$0^+, 1^+$	0	2.29	1^+			
7	2.408	1^+	0+2	87±15	2.410			2.41	1^+	2.411	0.26	
8	2.456		2	48±6	2.464					2.455	0.70	0.06
9	2.611 ^f			30±6						2.605	0.04	0.02
10	3.019 ^g	0^+	0	350±50	3.018 ^g	0^+	0			3.043 ^h		
11	3.702	1^+	0+2	290±30	3.701	$0^+, 1^+$		3.71	1^+			
12	3.819			50±25								
13	3.866	1^+	0+2	380±40				3.87	1^+			
14	4.698	1^+	0+2	180±25				4.69	1^+			
15	4.798	1^+	0+2	97±20				4.79	1^+			

^a Reference 7.

^b References 8-10.

^c Reference 11.

^d The energies for the levels 1 and 2 are taken from Refs. 5 and 6, those for levels 6, 7, 10, 11 and 13 are deduced from the present γ work.

^e The value is given at $\theta_{\text{lab}}=7^\circ$ for $L_{np}=0$ and 0+2, at $\theta_{\text{lab}}=18.5^\circ$ for $L_{np}=2$ and for L_{np} undetermined.

^f Two closely spaced levels.

^g Isobaric analog state corresponding to the 0^+ ground state in ^{48}Ti .

^h The angular distribution of the isobaric analog state does not have the shape characteristic of stripping.

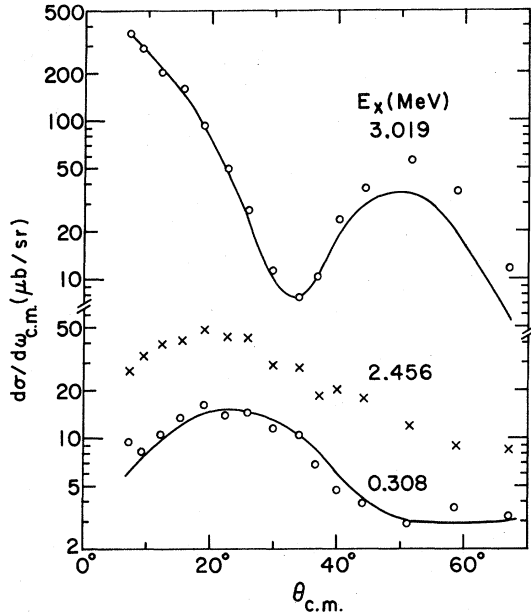


FIG. 2. Angular distribution of protons from the $^{46}\text{Ti}(^3\text{He}, p)^{48}\text{V}$ reaction. The top curve represents DWBA calculations for the 3.019-MeV state with angular momentum transfer $L_{np}=0$. Circles indicate the measured results. The lower curve shows a DWBA calculation for the 0.308-MeV state with $L_{np}=2$. Circles represent the experimental results.

reported cases (both in sd -shell nuclei),¹⁵ the population of 1^+ states has been found to take place by $L_{np}=0+2$ transfer. In the two atypical cases, the 1^+ final states may represent $(1d_{3/2}2s_{1/2})$ or $(2s_{1/2})^2$ configurations, both $J^\pi=1^+$, formed by the $n-p$ pair being captured by a 0^+ target nucleus. The first configuration will be formed only by an $L_{np}=2$ transfer, while the second configuration will be formed only by an $L_{np}=0$ transfer. Consequently, since similar configurations are not ex-

pected in the present case, the population of $J^\pi=1^+$ final states by the $(^3\text{He}, p)$ reaction on our $J^\pi=0^+$ target nucleus can safely be expected to take place by $L_{np}=0+2$ transfers. We therefore assign $J^\pi=1^+$ for the seven ^{48}V states whose proton angular distributions are shown in Fig. 3.

We would like to point out that one of the components ($E_x=4.583$ MeV) of the composite proton group mentioned in Sec. II A could be analyzed only at the three most forward angles. At the other angles this component is just barely above the background. This permitted us to determine an $L_{np}=0$ component for this state, but was not sufficient to distinguish between an $L_{np}=0$ and $L_{np}=0+2$ transfer. Hence this state has either $J^\pi=0^+$ or 1^+ with a cross section at 7° of 43 ± 20 $\mu\text{b}/\text{sr}$, smaller than any of the 0^+ or 1^+ states listed in Table I. The other component of the composite group has an angular distribution characteristic of $L_{np} \geq 2$. Hansen and Nathan¹⁰ report $J^\pi=1^+$ for a state at 4.58 MeV with a cross section not inconsistent with the one given above for the state at 4.583 MeV.

C. Particle- γ Coincidence Measurements

The γ decay of most of the levels shown in Figs. 2 and 3 have been studied by use of the $^{46}\text{Ti}(^3\text{He}, p\gamma)^{48}\text{V}$ reaction. The experimental arrangement was the same as that used in earlier investigations.¹⁶ A rolled ^{46}Ti target about $1 \text{ mg}/\text{cm}^2$ thick was bombarded by a 17-MeV ^3He beam. A 0.0075-cm gold foil placed directly behind the target stopped the beam so that a surface-barrier particle detector could be placed at 0° to the incoming beam. This placement is advantageous for the study of 0^+ and 1^+ states because it preferentially selects states populated with an $L_{np}=0$ contribution. The γ rays were measured with

TABLE II. The optical potentials and parameters used in the DWBA calculations, in which the potential for the unbound proton or ^3He is

$$V(r) = -Vf_v(r) - iWf_w(r) + 4i a_s W_s f'_s(r),$$

where

$$f_x = \{1 + \exp[(r - r_x A^{1/3})/a_x]\}^{-1}$$

and $f'_s = \partial f / \partial r$. The parameters of the potential in which the bound neutron and proton move are $a_v = 0.65$ fm and $r_v = 1.2$ fm. The program adjusts the real potential well until the binding energy is $E_n = \frac{1}{2}(|S_{np}| - E_x)$, where E_x is the excitation energy in the final nucleus and S_{np} is the separation energy of the $n-p$ pair. The values used were $S_{np} = -15.70$ MeV for the $T=1$ transfer and $S_{np} = -13.48$ MeV for the $T=0$. The potential contains a spin-orbit term.

Unbound particle	V (MeV)	a_v (fm)	r_v (fm)	W (MeV)	a_w (fm)	r_w (fm)	W_s (MeV)	a_s (fm)	r_s (fm)
p	53.6	0.61	1.217	0.	0.61	1.217	1.71	0.31	1.26
^3He	165.0	0.734	1.14	16.21	0.734	1.13	0	0.753	1.604

a 30-cm³ Ge(Li) detector placed at 100° to the ^3He beam.

A spectrum of particles in coincidence with all γ rays is shown in Fig. 4. The gold foil in front of the particle detector results in poor resolution (a few hundred keV, FWHM) for the proton groups but, of course, the good energy resolution in these coincidence measurements is provided by the γ detector. Most of the coincidences recorded are due to the $^{46}\text{Ti}(^3\text{He}, d\gamma)^{47}\text{V}$ and $^{46}\text{Ti}(^3\text{He}, np\gamma)^{47}\text{V}$ reactions, both of which have large cross sections but fortunately rather small Q values, so that the $(^3\text{He}, p\gamma)$ reaction for ^{48}V levels up to about 5-MeV excitation energy is free from γ rays resulting from the deexcitation of levels in ^{47}V . Some γ -ray spectra resulting from the decay of the isobaric analog state at 3.019 MeV and from the 1^+ states at 3.702 and 3.866 MeV are shown in Fig. 5. Each spectrum was measured in coincidence with the protons populating the level. The top spectrum in Fig. 5 is from the analog at 3.019 MeV, while the bottom one is from both the 3.702- and 3.866-MeV levels since the proton groups populating these states greatly overlap.

The γ rays emitted from the 1^+ states which we

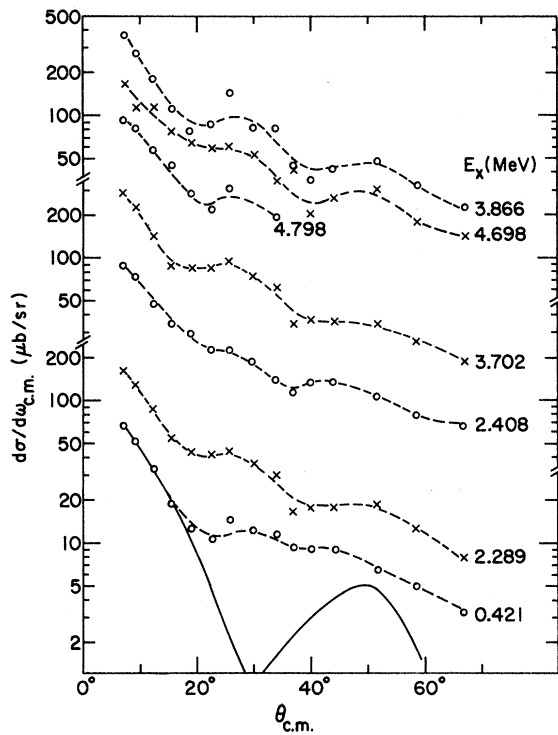


FIG. 3. Angular distributions of protons from the $^{46}\text{Ti}(^3\text{He}, p)^{48}\text{V}$ reaction which show the characteristic of $L_{np} = 0 + 2$ transfers. The solid curve at the bottom of the figure was calculated for $L_{np} = 0$. Circles and crosses represent the measured points; the dashed curves are guides for the eye.

could identify are listed in Table III and shown in Fig. 6(a). The γ -ray energies were determined to within ± 6 keV. The γ decays of the states at 2.289 and 2.408 MeV, which are also observed with the $(p, n\gamma)$ and $(d, n\gamma)$ reactions,⁵ agree with the results reported in this paper. The dotted line from the 2.408-MeV state indicates a very weak transition. The lines from the two highest-energy states are boxed because of our inability to distinguish between the two γ decays since, to within the uncertainty in the energies of the two states, the primary γ rays have the same energy. We could not associate any γ rays with the weakly-populated state at 4.583 MeV.

III. DISCUSSION

A. Level Scheme

The experimentally determined properties of states in ^{48}V , and the deduced spins and parities, are given in Tables I and IV. In Table V these results are compared with those obtained by shell-model calculations in which the valence neutrons and protons were assumed to occupy only the $f_{7/2}$ shell. The calculations shown in columns 3 and 4 in Table V were performed by Gloeckner and Lawson.¹⁸ The energies shown in column 3 of Table V were calculated with two-body interactions deduced¹ from recent experimental results on ^{42}Sc ; those in column 4 were calculated with the interactions derived from a number of experi-

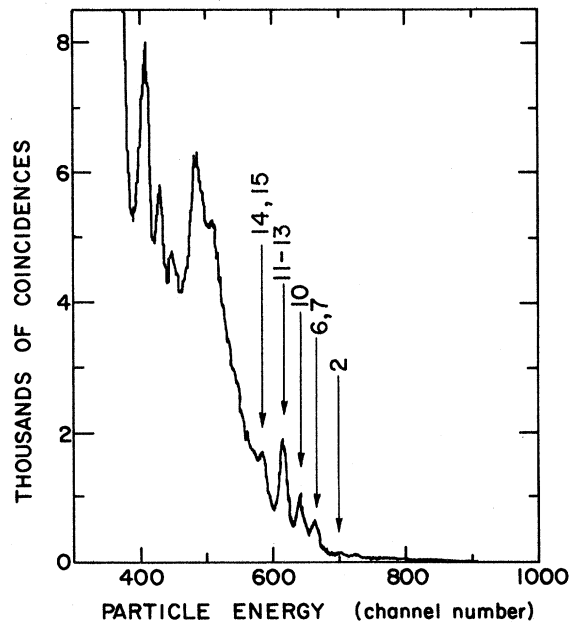


FIG. 4. $^{46}\text{Ti}(^3\text{He}, p)^{48}\text{V}$ spectrum of protons in coincidence with all γ rays. The peaks are labeled with level numbers from the list in Table I.

mentally well established ^{48}V levels and their spin assignments (those marked by daggers in column 2). The differences between the energies given in columns 3 and 4 are relatively small. This remains true if the calculations of column 4 are based on slightly different sets of levels.

The good agreement between the positions of the experimentally determined 1^+ levels and the calculated ones is of some interest since such agreement is not found in the case of ^{50}Sc , as Fleming *et al.*¹⁹ have pointed out. In the latter nucleus, the measured and calculated positions of the 1^+ states disagree strongly, even though all the configuration space of the $1f-2p$ shell is included in the calculation. The authors of Ref. 19 have taken this disagreement as an indication that some important degrees of freedom are not included in the calculations. However, the inclusion of these additional degrees of freedom are not necessary to secure good agreement between the calculated and measured energies for 1^+ states in ^{48}V .

B. γ Decays

A recent theoretical investigation¹ of states describable by the configuration $(\pi f_{7/2})^n (\nu f_{7/2})^{-n}$ makes an interesting prediction regarding $M1$ transitions among such states. The author introduces an operator called the signature operator which changes neutrons to protons and protons to neutrons. When the number of neutrons or neutron holes equals the number of protons the wave functions will be eigenfunctions of this operator and have eigenvalues $+1$ (positive signature) or -1 (negative signature). The matrix element for an $M1$ transition between states with opposite signatures is proportional to the difference between the magnetic moments of the proton and neutron while such transitions between states with the same signature is proportional to the sum of these magnetic moments. Hence one might expect $M1$ transitions between $(\pi f_{7/2})^n (\nu f_{7/2})^{-n}$ states with the same signatures to be weak. In fact the more

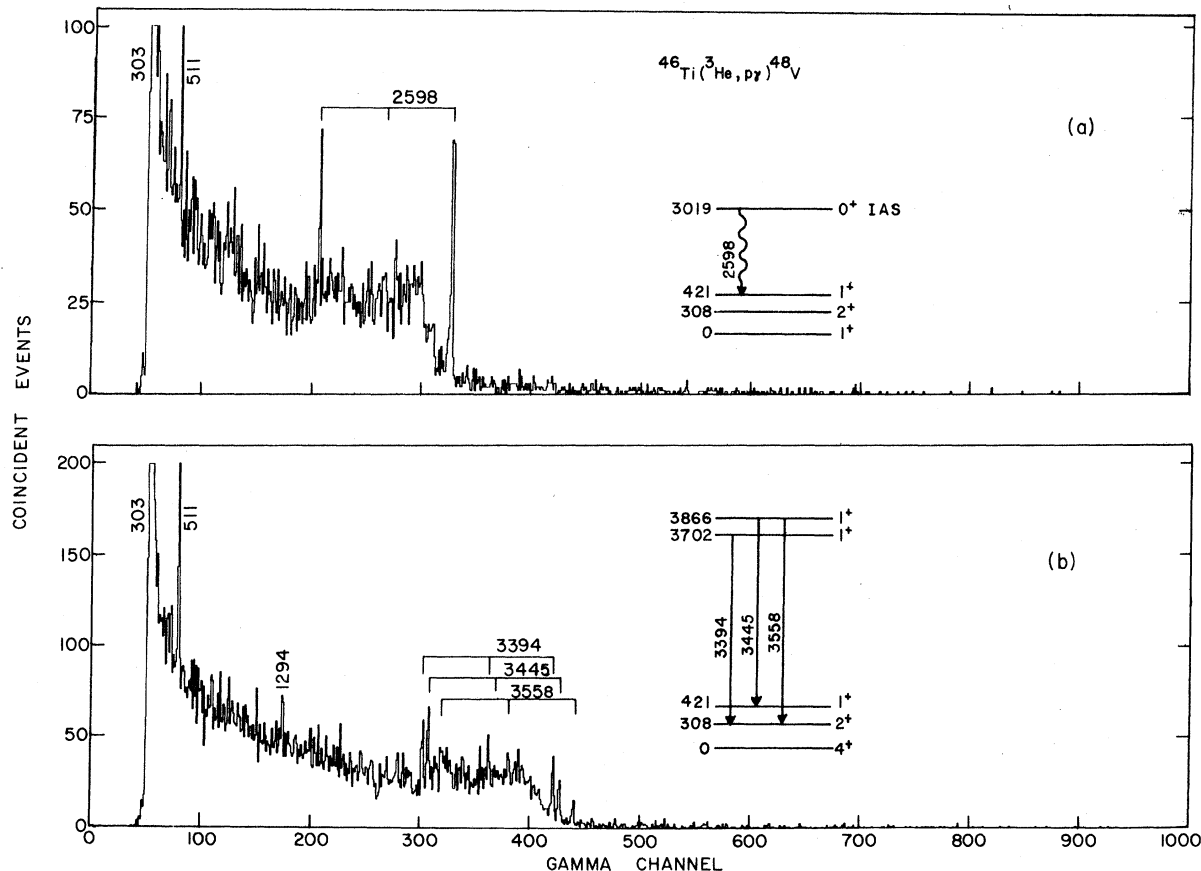


FIG. 5. Spectrum of γ rays in coincidence with the proton group populating the isobaric analog at 3.019 MeV (top curve) and in coincidence with the proton groups leading to the 3866- and 3702-MeV levels. The inserts represent the observed decay schemes.

TABLE III. The energies of the γ rays emitted from 1^+ and 0^+ states in ^{48}V .

E_x^{initial} (MeV) ^a	E_γ (MeV)	E_x^{final} (MeV)
2.289	1.981	0.308
2.408	1.989	0.421
3.019	2.598	0.421
3.702	3.394	0.308
3.866	3.445	0.421
3.866	3.558	0.308
4.693 ^b	4.368	0.325
4.797 ^b	4.368	0.428

^a The energies of all but the last two are deduced from the known energies of the first 1^+ and 2^+ states at 0.421 and 0.308 MeV, respectively, and the measured γ -ray energies.

^b The energy is taken from the spectrograph measurement. The error is about ± 15 keV.

detailed analysis¹ has shown that they are forbidden. In particular this selection rule should hold for the 1^+ states of configuration $(\pi f_{7/2})^3(\nu f_{7/2})^{-3}$ in the odd-odd cross-conjugate nucleus ^{48}V . Since the signature of neighboring 1^+ states changes

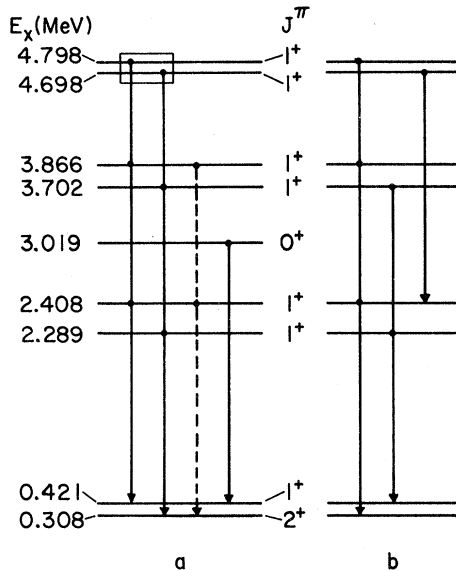


FIG. 6. The γ -ray decay of the 1^+ and 0^+ states in ^{48}V . (a) Decay scheme inferred from the present measurements. The dashed line represents a very weak transition. The box around the starting points of the transitions from the two top states indicates that the observed γ rays may come from either or both of these transitions; inaccuracy of the energies of the two top states does not allow a distinction between the two transitions. (b) Calculated decay scheme (Ref. 18). Only the strongest $M1$ transitions from the 1^+ states are indicated. $E2$ transitions are weaker and are not shown.

sign the expected γ decay of the 1^+ states in ^{48}V ¹⁸ is as shown in Fig. 6(b). Only the strongest transitions to the known 1^+ and 2^+ states are indicated. They are all $M1$ transitions. The observed γ decay is shown in Fig. 6(a). The second, fourth, and possibly the sixth 1^+ state decays to the first 2^+ state at 0.308 MeV; within the experimental error (which might lead to missing a 10–20% branch), we observe no other branch—in particular, none to the first 1^+ state at 0.421 MeV. The third, fifth, and possibly the seventh 1^+ states, however, decay strongly to the first 1^+ state at 0.421 MeV, with at most a small branch to the first 2^+ state at 0.308 MeV. The regularity described is similar to that expected from the Lawson calculation,¹ but the signature of the first 1^+ state seems to be wrong. This situation is unsatisfactory because changes in the two-body interactions have never resulted in a change of the signature of the first 1^+ state. Hence a theoretical explanation for this pattern remains to be found.

C. Differential Cross Sections

In the $(^3\text{He}, p)$ reaction, the total angular momentum transfer $J^\pi = 1^+$ indicated by the $L_{np} = 0 + 2$ angular distribution of the emerging protons (Fig. 3) is of interest since these $J^\pi = 1^+$ transfers seem to have especially large cross sections.¹⁹ In the present work, the sum of the 7° cross sections of all $^{48}\text{Ti}(^3\text{He}, p)^{48}\text{V}$ reactions populating 1^+ states at excitation energies up to about 5 MeV (Table I) is

$$I(L_{np} = 0 + 2) = \sum \frac{d\sigma}{d\Omega} (J^\pi = 1^+) = 1.3 \text{ mb/sr}.$$

This disagrees only slightly with the value 2.2 mb/sr measured¹⁰ at $\Theta = 3.75^\circ$, since the cross section for an $L_{np} = 0 + 2$ transfer is smaller at 7° than at 3.75° , as seen in Fig. 3. It is shown in Ref. 10 that $I(L_{np} = 0 + 2)$ is roughly the same for

TABLE IV. Recent spin assignment of levels in ^{48}V .

Reference 5 E_x (MeV)	J^π	Reference 17 E_x (MeV)	J^π	Reference 6 E_x (MeV)	J^π
0	4^+				
0.308	2^+			0.309	2^+
0.421	1^+			0.421	1^+
0.428	$5^{(+)}$	0.428	5^+	0.428	5^+
0.614	$4^{(+)}$	0.614	4^+		
0.627	$6^{(+)}$	0.627	6^+	0.628	6^+
0.765	$3^{(+)}$	0.765	3^+	0.775	$3^+, 5^+$
				1.100	$3^+, 5^+$
1.265	$5^{(+)}$	1.267	5^+	1.255	7^+

all even-even target nuclei with neutron numbers in the range $20 < N \leq 28$.

Moreover, in the $^{48}\text{Ca}(^3\text{He}, p)^{50}\text{Sc}$ reaction Fleming *et al.*¹⁹ measured the cross sections for the $J^\pi_{np} = 1^+$ transfers populating all the 1^+ states in ^{50}Sc and the cross section for the $J^\pi_{np} = 5^+$ transfer populating the 5^+ ground state and compared these with the cross sections obtained from DWBA calculations. They find that the experimental ratio of the sum of the cross sections for transfer to 1^+ states to the cross section for transfer to the 5^+ ground state is about 3 times as large as the corresponding theoretical ratio. They suggest that the reason the experimental value of $\sum (d\sigma/d\Omega)(J^\pi_{np} = 1^+)$ is larger than the calculated value may be that configurations from higher shells (probably $3s$ and $2d$ shells) participate in the 1^+ states. This admixture is expected to occur for all even-even target nuclei with $20 < N \leq 28$ since they all show about equally large cross sections for the $(^3\text{He}, p)$ reaction populating 1^+ states.¹⁰

One should note the contrast between these results for even-even target nuclei and that for an odd-even target with a neutron number in the range $20 < N \leq 28$. With the $L_{np} = 0 + 2$ transfers again recognized by the characteristic shapes of

TABLE V. Comparison of measured and calculated energies of some ^{48}V levels.

J^π	Excitation energy (MeV)		
	Exper. ^a	Calc. I ^b	Calc. II ^b
0^+	3.019 [†]	3.022	3.020
1^+	0.421 [†]	0.493	0.551
1^+	2.289 [†]	2.057	2.093
1^+	2.408 [†]	2.592	2.406
1^+	3.702 [†]	3.705	3.540
1^+	3.866 [†]	3.993	3.936
1^+	4.698 [†]	4.583	4.607
1^+	4.798 [†]	5.652	5.070
2^+	0.308 [†]	-0.132	-0.131
2^+	...	1.647	1.826
3^+	0.765 [†]	0.967	0.923
4^+	0.0	0.0	0.0
4^+	0.614 [†]	0.168	0.311
5^+	0.428 [†]	0.705	0.683
5^+	1.267	1.085	1.004
6^+	0.627 [†]	0.453	0.341
7^+	1.255	1.19	1.046

^a Results of present work and of Refs. 5, 6, and 17.

^b Calculations by Gloeckner and Lawson (Ref. 18). In Calc. I, the two-body interactions were deduced (Ref. 1) from recent measurements on ^{42}Sc ; in Calc. II, they were obtained from the well-established level energies and spins marked by [†] in column 2.

the angular distributions of the emerging protons,¹³ the summed differential cross section for the $^{45}\text{Sc}(^3\text{He}, p)^{47}\text{Ti}$ reaction is $I(L_{np} = 0 + 2) = \sum (d\sigma/d\Omega)(J^\pi_{np} = 1^+) = 0.25$ mb/sr—only about a fifth of the value we measured for the $^{46}\text{Ti}(^3\text{He}, p)^{48}\text{V}$ reaction. This cross section includes all ^{47}Ti states with $\frac{5}{2}^-$, $\frac{7}{2}^-$, or $\frac{9}{2}^-$ and energies up to 7.5 MeV.

Another striking difference between the $(^3\text{He}, p)$ reactions on ^{45}Sc and on the few measured even-even target nuclei is observed when the cross section for the $J^\pi = 0^+$ transfer indicated by the $L_{np} = 0$ angular distribution (upper curve in Fig. 2) is compared with those of the $J^\pi = 1^+$ transfers indicated by $L_{np} = 0 + 2$ distributions (Fig. 3). The $J^\pi = 0^+$ transfers populate analog and antianalog states^{13, 14} that lead to 0^+ states in the case of even-even target nuclei and to $\frac{7}{2}^-$ states in the case of the ^{45}Sc target. The values of $I(L_{np} = 0) = \sum (d\sigma/d\Omega)(J^\pi_{np} = 0^+)$, $I(L_{np} = 0 + 2)$, and the ratio $I(L_{np} = 0)/I(L_{np} = 0 + 2)$ —all measured at $\Theta = 7^\circ$ —are listed in Table VI, which also includes the bombarding energies. For the few selected nuclei tabulated here, the $L_{np} = 0$ strength is seen to vary only slightly, but the $L_{np} = 0 + 2$ strength is much smaller for the odd-even target nucleus ^{45}Sc than for the even-even targets.

This difference between the odd-even ^{45}Sc and the even-even target nuclei is even better demonstrated by the ratio $I(L_{np} = 0)/I(L_{np} = 0 + 2)$, which has the advantage of being independent of the measurements of absolute cross sections. This advantage is particularly important because recent studies^{4, 10, 20, 21} of the $(^3\text{He}, p)$ reaction have yielded differences between the cross sections—differences that are too large to be attributed to differences in bombarding energies and angles. As seen in Table VI, the ratio $I(L_{np} = 0)/I(L_{np} = 0 + 2)$ is about 5 times larger for ^{45}Sc than for the even-even target nuclei ^{46}Ti , ^{48}Ti , and ^{56}Fe .

As mentioned earlier Hansen and Nathan¹⁰ proposed that the large cross sections for $J^\pi = 1^+$ transfers ($L_{np} = 0 + 2$) to even-even target nuclei

TABLE VI. The $(^3\text{He}, p)$ transition strength for $L_{np} = 0$ and $L_{np} = 0 + 2$ orbital-angular-momentum transfers for some $1f2p$ -shell nuclei.

Final nucleus	^{47}Ti ^a	^{48}V ^b	^{50}V ^c	^{58}Co ^d
$E(^3\text{He})$ (MeV)	17.0	17.0	22.0	22.0
$I(L_{np} = 0)$ (mb/sr) _{c.m.}	0.34	0.35		0.24
$I(L_{np} = 0 + 2)$ (mb/sr) _{c.m.}	0.26	1.30		0.95
$I(L_{np} = 0)/I(L_{np} = 0 + 2)$	1.3	0.27	0.23	0.25

^a Reference 13.

^c Reference 16.

^b Present work.

^d Reference 20.

result from admixtures of higher-shell configurations. One would expect similar admixtures when using odd-even target nuclei. However, the relatively small strength of the $J^\pi_{np} = 1^+$ transfers to ^{48}Sc disagrees with this expectation. It is interesting to note that the strength for $J^\pi_{np} = 0^+$ transfers to ^{48}Sc is about the same as for the even-even target nuclei. Before firm conclusions can be drawn, more ($^3\text{He}, p$) reactions with odd-even target nuclei must be performed. Unfortunately only a few such nuclei are stable. The measurements are also complicated in that the analogs populated by the $J^\pi = 0^+$ transfer in the ($^3\text{He}, p$) reaction on odd-even target nuclei have high excitation energies—sometimes above the particle threshold. In contrast, those reached from even-even target nu-

clei are at considerably lower energies—an energy range in which the angular distributions of the observed levels can be measured with much greater accuracy.

ACKNOWLEDGMENTS

We are grateful to Dr. R. D. Lawson and Dr. D. Gloeckner for many helpful discussions and contributions and to F. G. Karasek of the Materials Science Division for preparing the target. We also thank Michelle Fleekey for help in reducing and analyzing the data. One of us (G. H.) wishes to thank the Western Michigan University Office of Research Services for partial support of this work through a faculty research grant.

[†]Work performed under the auspices of the U. S. Atomic Energy Commission.

^{*}Present address: Amoco Production Corporation, Houston, Texas 77001.

[‡]Also at Physics Department, Western Michigan University, Kalamazoo, Michigan 49001.

¹R. D. Lawson, Nucl. Phys. **A173**, 17 (1971).

²J. R. Erskine, in Argonne National Laboratory Reports ANL-7461, 1969 (unpublished), p. 7; ANL-7728, 1970 (unpublished), p. 43.

³J. R. Erskine and R. H. Vonderohe, Nucl. Instrum. Methods **81**, 221 (1970).

⁴J. W. Smith, L. Meyer-Schützmeister, T. H. Braid, P. P. Singh, and G. Hardie, Phys. Rev. C **7**, 1099 (1973).

⁵L. Samuelson, Bull. Am. Phys. Soc. **17**, 70 (1972), and private communication.

⁶R. B. Huber, C. Signorini, W. Kutschera, and H. Morinaga, Nuovo Cimento **15A**, 501 (1973).

⁷W. E. Dorenbusch, T. A. Belote, and J. Rapaport, Nucl. Phys. **A109**, 649 (1968).

⁸J. W. Smith, L. Meyer-Schützmeister, R. D. Lawson, T. H. Braid, and P. P. Singh, Bull. Am. Phys. Soc. **17**, 582 (1972).

⁹T. Caldwell, Ph. D. thesis, University of Pennsylvania, 1972 (unpublished); quoted in Ref. 10.

¹⁰O. Hansen and O. Nathan, Phys. Lett. **39B**, 419 (1972).

¹¹W. E. Dorenbusch, T. A. Belote, J. Rapaport, and K. G. Nair, Nucl. Phys. **A112**, 385 (1968).

¹²The calculations have been performed with the code

TWOPAR. We are grateful to B. F. Bayman for having made this code available to us.

¹³L. Meyer-Schützmeister, J. W. Smith, G. Hardie, H. Siefken, K. J. Knöpfle, M. Rogge, and C. Mayer-Böricke, Nucl. Phys. **A199**, 593 (1973).

¹⁴R. R. Betts, H. T. Fortune, J. D. Garrett, R. Middleton, D. J. Pullen, and O. Hansen, Phys. Rev. Lett. **26**, 1121 (1971); T. Caldwell, D. J. Pullen, T. J. Mulligan, and O. Hansen, Nucl. Phys. **A175**, 31 (1971).

¹⁵R. R. Betts, H. T. Fortune, D. J. Pullen, and B. H. Wildenthal, in *Symposium on Two-Nucleon Transfer and Pairing Excitations*, Argonne National Laboratory Physics Division Informal Report No. PHY-1972H, 1972 (unpublished), p. 342.

¹⁶J. W. Smith, Ph. D. thesis, Indiana University, 1971 (unpublished); J. W. Smith, L. Meyer-Schützmeister, T. H. Braid, P. P. Singh, and G. Hardie, Phys. Rev. C **7**, 1099 (1973).

¹⁷B. A. Brown, J. M. McDonald, K. A. Snover, and D. B. Fossan, Bull. Am. Phys. Soc. **17**, 933 (1972).

¹⁸D. Gloeckner and R. D. Lawson, private communication.

¹⁹D. G. Fleming, R. A. Broglia, K. Abdo, O. Nathan, D. J. Pullen, B. Rosner, and O. Hansen, Phys. Rev. C **5**, 1356 (1972).

²⁰G. Hardie, T. H. Braid, L. Meyer-Schützmeister, and J. W. Smith, Phys. Rev. C **7**, 2466 (1973).

²¹L. L. Lynn, R. C. Schaller, D. A. Barbour, and T. A. Belote, Nucl. Phys. **A182**, 272 (1972).